tumor treatments (another scenario in which the immune system is subject to chronic antigen exposure) (*6*, *10*), and its therapeutic potential is appealing. At the same time, the capacity of IL-21 to enhance the $CD8^+$ T cell response may come at a cost: Treating chronic LCMV-infected $CD4^+$-deficient animals with IL-21 led to severe sickness (*4*). Hence, prospective therapeutic use of IL-21 will need to be finely tuned.

$CD4^+$ T cell help is also important for the $CD8^+$ T cell response to various acute infections (*2*). In such responses, lack of $CD4^+$ help (or lack of IL-2 sensitivity) typically has minimal impact on $CD8^+$ T cell priming, but leads to a failure of memory $CD8^+$ T cells to mount a response to subsequent infection by the same pathogen (*2*). The current reports find no effect of IL-21 or IL-21R deficiency on the primary $CD8^+$ T cell responses to various acute infections (*3*–*5*), and in one study, memory $CD8^+$ T cell responses to LCMV were intact (*5*). Such data strongly suggest that IL-21 is a key element of $CD4^+$ T cell help in $CD8^+$ T cell responses to chronic but not acute infections. Furthermore, the elevated and sustained production of IL-21 (but not IL-2) in $CD4^+$ T cells from chronically infected animals contrasts with the sustained capacity for IL-2 (but not IL-21) synthesis by $CD4^+$ T cells following acute infection (*3*). Thus, the basis by which $CD4^+$ T cells help the $CD8^+$ T cell responses may change depending on the nature of the infection. IL-21 appears to induce a unique differentiation pathway in activated $CD8^+$ T cells (*6*, *10*, *11*), potentially equipping them to better clear virus during a chronic infection. Whether the IL-21–producing $CD4^+$ T cells also function as follicular helper T cells or T_H17 cells during chronic viral infection is unclear [although Fröhlich *et al*. argue against T_H17 involvement (*5*)]. Regardless, these studies suggest a key role for IL-21 in mediating $CD4^+$ help when it's needed most.

References

1. H. Shin, E. J. Wherry, *Curr. Opin. Immunol*. **19**, 408 (2007).
2. M. A. Williams, M. J. Bevan, *Annu. Rev. Immunol*. **25**, 171 (2007).
3. H. Elsaesser, K. Sauer, D. G. Brooks, *Science* **324**, 1569 (2009); published online 7 May 2009 (10.1126/science.1174182).
4. J. S. Yi, M. Du, A. J. Zajac, *Science* **324**, 1572 (2009); published online 14 May 2009 (10.1126/science.1175194).
5. A. Fröhlich *et al*., *Science* **324**, 1576 (2009); published online 28 May 2009 (10.1126/science.1172815).
6. R. Spolski, W. J. Leonard, *Annu. Rev. Immunol*. **26**, 57 (2008).
7. J. S. Silver, C. A. Hunter, *Immunity* **29**, 7 (2008).
8. R. Zeng *et al*., *J. Exp. Med*. **201**, 139 (2005).
9. M. T. Kasaian *et al*., *Immunity* **16**, 559 (2002).
10. C. S. Hinrichs *et al*., *Blood* **111**, 5326 (2008).
11. K. A. Casey, M. F. Mescher, *J. Immunol*. **178**, 7640 (2007).

10.1126/science.1176487

CHEMISTRY

Extracting Potentials from Spectra

An analysis of the spectra of the elusive beryllium dimer, aided by ab initio calculations, characterizes the molecule near its dissociation limit.

Peter F. Bernath

For most elements, we know whether they can form a diatomic molecule, especially for light atoms that have few electrons and can be treated readily by theory. But for one such light element, surprises are still in store. For most of the 20th century, experimental and theoretical studies agreed that the beryllium dimer (Be_2) did not exist. The Be atom has filled electron shells and—like the inert gases such as helium—was expected to form at most a weak van der Waals dimer at very large internuclear distances. Yet, as shown experimentally by Merritt *et al*. on page 1548 of this issue (*1*), Be_2 does exist and has a relatively short bond (2.45 Å), relative to the anticipated van der Waals complex with a bond length of about 5 Å. Its unusually flat potential curve limits the number of vibrational levels and provides the rare opportunity to study the highest vibrational state of a molecule just at its dissociation limit.

Experiments with beryllium are difficult because the metal is refractory (it has a low vapor pressure even at very high temperatures) and because beryllium-containing compounds are generally extremely toxic. However, Be vapor can be created through laser ablation of a Be metal target. Rapid cooling of the vapor during supersonic expansion through an orifice into vacuum allows preparation of the dimer. The rovibrational states of the dimer are then probed with a double-resonance method: One laser excites the molecule into an excited electronic state where the atoms are still bound; stimulated emission pumping (*2*) by a second laser returns the molecule back into each of the bound vibrational levels of the ground state.

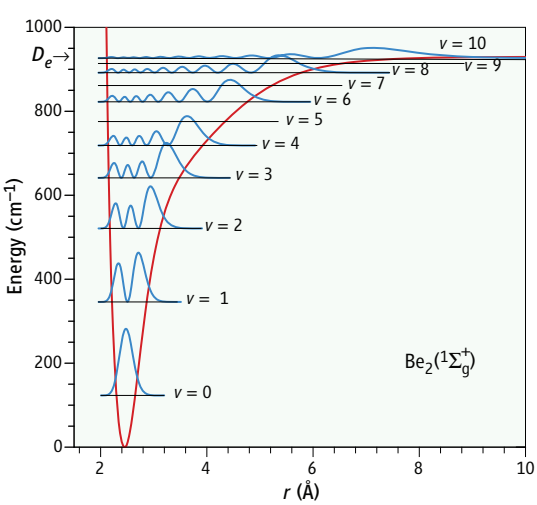

Shallow potentials with deeper implications. The potential energy function for Be_2 as a function of interatomic distance r was determined by Merritt *et al*. from a fit to the experimental observations. The levels become more congested as the energy nears the dissociation limit D_e. The bound vibrational energy levels and the square of the vibrational wave functions were calculated by LeRoy with his program LEVEL (*6*).

The data analysis performed by Merritt *et al*. is noteworthy because it allows a better connection to theory than standard methods. Vibration-rotation energy levels are usually reduced to spectroscopic constants that are parameters in a power series expansion that uses the relevant quantum numbers of the states (*3*, *4*). However, an excessively large number of expansion terms are needed, particularly for a potential with an unusual shape such as Be_2, and these fitting parameters have lost their physical meaning. In contrast, a parameterized potential function (see the figure) requires far fewer fitting parameters and makes a direct connection with ab initio quantum chemistry.

Merritt *et al*. adopted a more powerful analysis method that bypassed traditional constants in favor of a parameterized potential energy function obtained from a direct fit of the energy levels using the vibration-rotation Schrödinger

Department of Chemistry, University of York, Heslington, York, YO10 5DD, UK. E-mail: pfb500@york.ac.uk

equation. LeRoy has been one of the pioneers of this modern quantum mechanical approach, and the authors used his freely available computer code (*5*, *6*).

With only eight electrons, Be_2 has attracted and challenged quantum chemists for nearly 80 years. Ab initio quantum chemistry solves the electronic Schrödinger equation to obtain the interaction energy for a series of molecular geometries. Within the Born-Oppenheimer approximation, which separates fast electronic motion from slower vibration-rotation nuclear motion, these electronic energies are used to construct the potential energy function that is then used to solve the vibration-rotation Schrödinger equation. It is now even possible to deal with the breakdown of the Born-Oppenheimer approximation in both experiment (*7*) and ab initio theory (*8*).

Quantum chemistry attributes the formation of the Be–Be bond and the unusual potential shape to the inclusion of more and more p character in the valence orbitals as the atoms approach each other (*9*). The p orbitals are more directional than the s orbitals that describe the isolated atoms. The comparison between the experimentally derived potential of Merritt *et al*. and modern high-quality ab initio potentials such as those calculated in (*9*, *10*) is reasonable at the moment but definitely not perfect (*11*), with noticeable differences in the internuclear distance and in the dissociation energy.

It is experimentally challenging to measure the entire range of vibrational levels and locate the last bound level at $v = 10$, which has a binding energy of only a few wave numbers. Indeed it is even possible that there is another vibrational level with $v = 11$ that is bound by a tiny fraction of a wave number. As can be seen from the square of the wave function, which gives the probability distribution, the molecule spends nearly all of its time at a large internuclear separation of 7 Å for $v = 10$. The application of stimulated emission pumping and the availability of a suitable excited electronic state allowed Merritt *et al*. to map out the Be_2 levels.

Spectroscopic observations often focus on the lowest few vibrational levels of a potential because they are easier to observe and calculate, but modern computational and experimental methods—such as interactions seen in cold atom trapping (*12*)—can provide information on the last few levels near dissociation. In some cases [for example, MgH (*13*)], it is only the combination of modern potential fitting methods with high-quality observations that enables the last few bound levels to be located in the forest of stronger lines. The full characterization of all bound levels with experimental precision for small molecules such as water is still a distant goal, but the first steps with, for example, H_2 (*14*), MgH (*13*), and now Be_2, are important landmarks on the way.

References and Notes

1. J. M. Merritt, V. E. Bondybey, M. C. Heaven, *Science* **324**, 1548 (2009).
2. C. E. Hamilton, J. L. Kinsey, R. W. Field, *Annu. Rev. Phys. Chem*. **37**, 493 (1986).
3. J. L. Dunham, *Phys. Rev.* **41**, 721 (1932).
4. P. F. Bernath, *Spectra of Atoms and Molecules* (Oxford Univ. Press, Oxford, ed. 2, 2005).
5. R. J. LeRoy, J. Y. Seto, Y. Huang, "DPotFit; a computer program for fitting diatomic molecular spectral data to potential energy functions," University of Waterloo Chemical Physics Research Report CP-662R (2006).
6. See http://leroy.uwaterloo.ca/programs.html.
7. R. J. Le Roy *et al*., *J. Chem. Phys*. **123**, 204304 (2005).
8. D. W. Schwenke, *J. Chem. Phys*. **118**, 6898 (2003).
9. J. M. L. Martin, *Chem. Phys. Lett*. **303**, 399 (1999).
10. R. J. Gdanitz, *Chem. Phys. Lett.* **312**, 578 (1999).
11. V. Spirko, *J. Mol. Spectrosc.* **235**, 268 (2006).
12. J. M. Hutson, P. Soldán, *Int. Rev. Phys. Chem*. **25**, 497 (2006).
13. A. Shayesteh *et al*., *J. Phys. Chem.* A **111**, 12495 (2007).
14. I. Dabrowski, *Can. J. Phys*. **62**, 1639 (1984).

15. I thank R. J. LeRoy for making the figure and for his comments. Financial support was provided by the UK Engineering and Physical Sciences Research Council.

10.1126/science.1175751

NEUROSCIENCE

Bridging the Gap and Staying Local

Imaging with fluorescence reporters reveals the molecular nature of long-term memory storage at stimulated synapses.

Martin Korte

Long-term memory storage requires the transcription of specific genes in neurons (*1*). It also requires that the proteins encoded by these transcripts localize to regions in the neurons that forge the communicative neuronal connections, or synapses (*2*). Yet, how do gene products generated in the neuronal cell body (soma) "know" to which of all the neuron's synapses (up to 30,000) they have to be targeted? Two reports, by Wang *et al.* (*3*) on page 1536 of this issue and by Okada *et al.* (*4*), explore how long-lasting memory can be implemented at specific synapses.

One solution that has been debated is the tagging (or capture) hypothesis (*5*, *6*). The so-called synaptic tag serves as a molecular marker that targets synaptic plasticity-related proteins only to previously activated synapses. Generally available proteins would be transported into the activated synapses only after stimulation (*4*). Alternatively, the synaptic tag could spatially restrict new protein synthesis (local translation) at stimulated synapses (*7*, *8*). However, until now, there has been no direct evidence showing that specific messenger RNAs (mRNAs) undergo locally restricted translation at stimulated synapses only during long-lasting (transcription-dependent) synaptic plasticity.

To approach this problem, Wang *et al*. cultivated sensory and motor neurons of the sea slug *Aplysia californica* (a model system for studying synaptic plasticity) (*1*). This monosynaptic connection is a central part of the gill-withdrawal reflex in *Aplysia*. Multiple applications of the neurotransmitters serotonin or Phe-Met-Arg-Phe-NH_2 (FMRFamide) leads to long-term facilitation or depression of synaptic transmission, respectively, two effects that control memory storage. To monitor local translation of mRNA during long-lasting synaptic plasticity, Wang *et al*. generated an elegant molecular tool using mRNA that encodes sensorin, a sensory neuron–specific peptide neurotransmitter. Sensorin mRNA localizes to distal neuronal processes (neurites) and is abundant at synapses. Its translation to protein is necessary for serotonin-induced long-term facilitation. The authors fused the 5′ and 3′ untranslated regions of sensorin mRNA to the region of mRNA encoding dendra2, a fluorescent protein (*9*). Dendra2 switches its fluorescence irreversibly from green to red after illumination by ultraviolet light. The authors first converted dendra2 to red fluorescence by ultraviolet irradiation. Afterward, any green dendra2 detected represents newly produced protein via local translation (after the soma was cut off). Wang *et al.* show that green dendra2 became visible only at synapses that demonstrated long-term facilitation, but not at unstimulated synapses, nor when long-term depression was induced.

Zoological Institute, Division of Cellular Neurobiology, TU Braunschweig, D-38106 Germany. E-mail: m.korte@tu-bs.de